Polarization and Wide Incident Angle Insensitive Metal Free Superwideband Absorber For Terahertz and Infrared Spectrum

SARTHAK SINGHAL (sarthak.ece@mnit.ac.in)
Malaviya National Institute of Technology Jaipur https://orcid.org/0000-0002-1160-6150

Research Article

Keywords: Absorption bandwidth, infrared frequency spectrum, metal free absorber, superwideband absorber, terahertz applications, wide incident angle insensitive

Posted Date: March 22nd, 2022

DOI: https://doi.org/10.21203/rs.3.rs-1366608/v2

Abstract

A circular slot loaded octagonal metal free graphite based absorber for superwideband applications at terahertz and infrared spectrum is proposed. The absorber comprises a circular slot loaded octagonal graphite slab at the top layer, silicon dioxide as substrate and square graphite slab as the bottom layer. This absorber is operating over a frequency spectrum of 6 THz to more than 80 THz (ratio bandwidth of > 12:1 and fractional bandwidth of > 172.093%) for absorption more than 90% with unity peak absorption. The absorber dimensions are 5 μm × 5 μm × 7.04 μm. The thickness of the substrate is only ~ λo/26 and the periodicity of absorber is ~ λo/10 at 6 THz. The performance of the absorber is found to be insensitive to changes in polarization angle (Φ). Furthermore, the performance of the absorber is observed to be unaffected by incident angle (θ) variations from 0^o to 60^o. The metal-free geometry along with insensitiveness to Φ and $0^o \leq θ \leq 60^o$ makes the proposed absorber suitable for compact terahertz/infrared micro/nanoscale systems.

I. Introduction

Terahertz (THz) spectrum has received much interest from academia and industry in the last two decades for its vast applications in communication, imaging, medical, radar, sensing, spectroscopy, and other fields. The field of absorbers has been determined to be the most practical use of the THz spectrum. Researchers have recently reported several single and multilayered geometry-based terahertz absorbers having narrowband, multi-band, wideband, and frequency-dependent reconfigurable performance [1–34]. Different techniques leading to the excitation of multiple resonances are used to design multi-band absorbers. The merging of these multiple resonances leads to wideband performance. Multilayered or multiple stacked systems provide wide bandwidth; however, they are challenging to implement. The easy to implement single layer structures provide limited operating frequency range. Therefore, a major challenge is to design a broadband absorber having single layer of substrate without any stacking of metallic/graphene layers.

Another challenge faced during absorber designing is the limited performance at higher frequencies due to the metals' limited electrical properties and high-temperature sensitivity, which is mainly responsible for incident power absorption in metal/dielectric multi-layered absorbers [27, 28]. Few researchers have reported absorbers based on vanadium oxide, a temperature-sensitive & phase change material [21, 29]. They provide desired wideband performance even at high temperatures, but these high temperatures affect the functioning of other nano-scale components. All the above-discussed broadband absorbers have complex fabrication techniques, thick geometries, and temperature-dependent performance. Thus, there is a need to design broadband absorbers whose fabrication is easy, the substrate thickness is negligible, and the performance is temperature independent. According to the available literature, metal-free absorbers like graphite/dielectric-based absorbers and semiconductor grating-based absorbers have provided temperature-independent performance [26, 30, 31]. The major reason for the usage of graphite in flexible electronics components like THz antennas and high-frequency absorbers is its better temperature stability [21]. These broadband metal-free absorbers can cover only a small portion of the terahertz spectrum. The future requirements require the coverage of both terahertz and infrared spectrum.

This paper presents the design and analysis of a metal-free graphite/dielectric-based super wideband absorber. The combination of circular slot-loaded octagonal graphite slab, silicon dioxide dielectric material, and square graphite slab resulted in an operating frequency range from 6 THz to more than 80 THz with the absorption of more than 90% for the normal incidence of electromagnetic waves. In two frequency bands of 7.85–13.05 THz and 22.47 THz to more than 80 THz, the absorption is found to be more than 95%. In the frequency spectrum of 25.35–28.71 THz, 44.68–74.65 THz, and 79.52 THz to more than 80 THz, the absorption is more than 99%. The proposed absorber's overall volume is significantly lesser than several dielectric, metamaterial, and grating-based structures. The advantageous features of planar metal-free geometry with miniaturized dimensions, low volume, insensitivity to polarization angle, and wide incident angle range make this absorber compatible with the future nanoscale super wideband terahertz and infrared systems.

Ii. Absorber Design

The proposed antenna geometry, shown in Fig. 1, is a three layered structure. In the proposed absorber, a 1.54 μm thick silicon dioxide substrate is sandwiched between two graphite slabs. The top graphite slab is octagonal in shape. It is loaded with a central circular slot. During the simulation of the proposed absorber structure by using finite integration technique (FIT)-based CST Microwave Studio (CST MWS), periodic boundaries are fixed along x- and y-axis. Along the z-axis i.e. transmission direction, open boundary conditions are fixed. This absorber is designed in three stages i.e. initially only graphite ground is analyzed. In second stage, the combination of graphite ground and substrate is analyzed. In the last stage, the circular slot loaded octagonal graphite, substrate material and graphite ground plane are analyzed together.

Iii. Results And Discussion

The magnitudes of reflectance (S_{11}) and transmittance (S_{21}) for all absorber designing stages are shown in Fig. 2. It is observed that for each stage the magnitude of transmittance is almost zero i.e. $\left|S_{21}\right| \cong 0$. The reflectance for first stage is decreasing linearly from 1 to 0.7 in the frequency range of 1 to 80 THz without any resonance. For second stage, two resonance at the frequencies of 22.79 and 69.85 THz with $|S_{11}|$ of 0.55 and 0.23 are observed. In the last stage, the reflectance is observed to be sharply decreasing from 1 to 0.1 with three resonances. For the frequency range of 6.33 THz to more than 80 THz, the reflectance magnitude is less than 0.3. By using these values of reflectance and transmittance in the absorption equation, $A = 1 - \left|S_{11}\right|^2 - \left|S_{21}\right|^2$ the values of absorption are calculated for each designing stage. Since $|S_{21}|=0$, therefore the above equation is reduced to $A = 1 - \left|S_{11}\right|^2$. The absorption values for each designing stage are shown in Fig. 2 (c). For first stage, a maximum absorption of 50% is achieved. In second stage, two peaks having absorption of 70% and 95% are observed at resonance frequencies. In the last stage, absorption of more than 90% is achieved in the frequency spectrum of 6THz to more than 80 THz. Figure 3 illustrates a good agreement between the absorption in both modes i.e. transverse electric (TE) and magnetic (TM) for the proposed absorber.

To analyze the polarization sensitiveness of this absorber, the polarization angle (Φ) is varied from 0^o to 90^o. Due to the geometrical symmetry, this absorber is insensitive to the variations in polarization angle as shown in Fig. 4.

Table 1 illustrates that the proposed absorber has widest bandwidth (6 THz to more than 80 THz) along with minimum volume of 176 μm^3 among the compared structures. The proposed absorber is covering terahertz frequency spectrum from 6–10 THz and infrared region from 10 THz to more than 80 THz whereas the operating band of other absorbers is covering only a narrow portion of the terahertz spectrum. In addition to this, this absorber is polarization angle and wide incident angle insensitive.

Table 1
Comparison of proposed absorber with other absorber structures

Reference	Geometry	Material	Unit cell dimensions (μm × μm × μm)	Absorption operating range in THz / (Absorption criteria in %)	% BW	Polarization insensitivity	Incident Angle (θ°) (for A > 90%)	
							TE	TM
[6]	Multiple square patches resonators	Copper and SiO2	20×20×0.7	6.23–7.08 THz / (80) 6.24–7.04 THz / (90)	12.772 12.048	yes	-	-
[7]	Multiple stacked bars resonators	Polyimide and Gold bars	Not available	0.8-1.368 THz / (80) 0.8 to 1.28 THz / (90)	52.399 46.154	no	40	40
[8]	Hybrid Structure	Polyimide and Gold	376×376	0.13 THz(80) 0.22–0.33 THz / (90)	0 40	Yes	45	45
[9]	Sectional asymmetric structure	Au and Si3N4	19.4×19.4	4.6–5.1 THz / (80)	10.309	No	30	30
[10]	Fractal cross resonators	Polyimide and Gold	40×40×11.24	3.01–4.84 THz / (80)	46.624	-	45	45
[11]	Stacked cross resonators	Parylene, Gold, Aluminium and Silicon	80×80×12	7.1-8 THz / (80)	11.921	-	-	-
[12]	Nested circular rings	Copper and polyimide	30×30×10.2	1.6–2.6 THz / (80) 0.896 THz / (90)	47.619 0	Yes	60	60
[13]	Truncated pyramid structure	SU8 polymer and gold	95×95×21	0.75–1.5 THz / (80)	66.667	Yes	30	70
[14]	Grating structure	Doped Silicon	100×100×500	0.58–2.58 THz / (90)	126.582	Yes	45	55
[15]	Multiple I-shaped strips	Polyimide and gold	78×78×8.5	0.87–0.97 THz / (80)	10.87	Yes	60	60
[16]	Pythagorean tree fractal structure	Polyimide and gold	69×69×22.2	7.5–10 THz / (80)	28.571	No	0	0
[17]	Multiple diamond array	Dielectric and diamond	170×170×310	1.3 THz / (90)	95.65	No	45	40

Reference	Geometry	Material	Unit cell dimensions (µm × µm × µm)	Absorption operating range in THz / (Absorption criteria in %)	% BW	Polarization insensitivity	Incident Angle (θ^o) (for A > 90%)	
							TE	TM
[18]	Slot loaded rectangular structure	Metal and Dielectric	88×88×14	1.3–2.7 THz / (90) 1.24–2.86 THz / (50)	70	No	-	-
[19]	three-layer structure, comprising square-, cross-, and circular-shaped	Metal, dielectric and grapheme	58×58×50	0.55–3.12 THz / (90)	140	Yes	15	45
[20]	square ring and multiple T-shaped resonators	Metal and dielectric	120×120×22	4.904–6.632 THz / (90)	29.95	Yes	0	0
[21]	L shaped resonators	VO2 and dielectric	50×50×26	1.2–3.2 THz / (90)	90.90	No	50	50
[22]	Cross shaped resonators	Metal and dielectric	225×225×325	0.65–2.45 THz / (90)	116.12	Yes	40	40
[23]	Rectangular ring loops	Metal,dielectric and nitride	70×70×24	1.17–2.99 THz / (90)	87.5	Yes	30	30
[24]	wheel hub-like	Metal	200×200×90	1.6-5 THz / (90)	103	Yes	45	70
[25]	Multiple circular resonators	Metal, dielectric and grapheme	80×24×28	1.6–3.2 THz / (90)	63.91	No	50	-
[26]	Annular ring	Dielectric and graphite	85×85×50.2	0.65–3.03 THz / (90)	129.34	Yes	50	50
Proposed Absorber	Octagonal Annular Ring	Dielectric and graphite	5×5×7.04	6 THz to more than 80 THz (90)/ 4.8 THz to more than 80 THz (80)	> 172.093	Yes	60	60

Iv. Conclusion

A superwideband absorber based on dielectric and graphite material for operation at terahertz and infrared frequency spectrum is investigated. It has an operating bandwidth of more than 74 THz starting from 6 THz for absorption more than 90%. Due to the presence of only graphite as conducting material, this absorber will be insensitive to the temperature variations. Since the absorber geometry is symmetrical, it has insensitiveness to polarization angles. It is insensitive to a wide range of incident angle variations upto 60^{o}.

Declarations

*** Ethics approval:** Not Applicable

*** Consent to participate:** Not applicable

* Consent for publication: Not applicable

* Availability of data and materials: Data sharing not applicable to this article as no datasets were generated or analysed during the current study.

* Competing interests: The author has no relevant financial or non-financial interests to disclose.

* Funding: The authors declare that no funds, grants, or other support were received during the preparation of this manuscript.

* Authors' contributions: The sole author Sarthak Singhal has contributed to the study conception, design, material preparation, data collection, analysis and writing of the manuscript.

* Acknowledgements: Not applicable

* Authors' information (optional).
Please include the sub-sections below of Compliance with Ethical Standards section.

* Disclosure of potential conflicts of interest: The author has no relevant financial or non-financial interests to disclose.

* Research involving Human Participants and/or Animals: Not applicable

* Informed consent: Only single author is there

References

1. A. Mohanty, O. Acharya, B. Appasani, and S. Mohapatra, “A multi-band terahertz metamaterial absorber based on a Π and U-shaped structure,” Photonics and Nanostructures - Fundamentals and Applications, vol. 32, pp. 74–80, 2018.
2. R. M. H. Bilal, M. A. Baqir, P. K. Choudhury, M. Karaaslan, M. M. Ali, O. AltIntas, A. A. Rahim, E. Unal, and C. Sabah, “Wideband Microwave Absorber Comprising Metallic Split-Ring Resonators Surrounded With E-Shaped Fractal Metamaterial,” IEEE Access, vol. 9, pp. 5670–5677, 2021.
3. M. R. Soheilifar and R. A. Sadeghzadeh, Design, fabrication and characterization of stacked layers planar broadband metamaterial absorber at microwave frequency," *AEU-Int. J. Electron. Commun.*, vol. 69, no. 1, pp. 126_132, Jan. 2015.;
4. D.-E.Wen, X. Huang, L. Guo, H. Yang, S. Han, and J. Zhang, Quadrupleband polarization-insensitive wide-angle metamaterial absorber based on multi-layer structure," *Optik*, vol. 126, nos. 9_10, pp. 1018_1020,May 2015.
5. Zhao J and Cheng Y (2016) A high-efficiency and broadband reflective 90° linear polarization rotator based on anisotropic metamaterial. Applied Physics B: Photophysics and Laser Chemistry 255, 1–7.
6. Y. Cheng, Y. Nie, and R. Gong, “A polarization-insensitive and omnidirectional broadband terahertz metamaterial absorber based on coplanar multi-squares films,” Opt. Laser Technol.**48**, 415–421 (2013).

7. S. Liu, H. Chen, and T. J. Cui, “A broadband terahertz absorber using multi-layer stacked bars,” Appl. Phys. Lett.**106**(15), 151601 (2015).
8. Y. L. U. Uying, J. L. I. Ining, S. H. Z. Hang, and J. I. S. Un, “Polarization-insensitive broadband terahertz metamaterial absorber based on hybrid structures,” Appl. Opt.**57**(21), 6269–6275 (2018).
9. C. Gong, M. Zhan, J. Yang, Z. Wang, H. Liu, Y. Zhao, and W. Liu, “Broadband terahertz metamaterial absorber based on sectional asymmetric structures,” Sci. Rep.**6**(1), 32466–32473 (2016).
10. M. Kenney, J. Grant, Y. D. Shah, I. Escorcia-Carranza, M. Humphreys, and D. R. S. Cumming, “Octave-Spanning Broadband Absorption of Terahertz Light Using Metasurface Fractal-Cross Absorbers,” ACS Photonics**4**(10), 2604–2612 (2017).
11. D. Jia, J. Xu, and X. Yu, “Ultra-broadband terahertz absorption using bi-metasurfaces based multiplexed resonances,” Opt. Express**26**(20), 26227–26234 (2018).
12. W. Pan, X. Yu, J. Zhang, and W. Zeng, “A Novel Design of Broadband Terahertz Metamaterial Absorber Based on Nested Circle Rings,” IEEE Photonics Technol. Lett.**28**(21), 2335–2338 (2016).
13. J. Zhu, Z. Ma, W. Sun, F. Ding, Q. He, L. Zhou, and Y. Ma, “Ultra-broadband terahertz metamaterial absorbear,” Appl. Phys. Lett.**105**(2), 021102 (2014).
14. Y. Peng, X. Zang, Y. Zhu, C. Shi, L. Chen, B. Cai, and S. Zhuang, “Ultra-broadband terahertz perfect absorber by exciting multi-order diffractions in a double-layered grating structure,” Opt. Express**23**(3), 2032 (2015).
15. L. Huang, D. R. Chowdhury, S. Ramani, M. T. Reiten, S. Luo, A. J. Taylor, and H. Chen, “a broad and flat high absorption band,” Opt. Lett. 37(2), 154–156 (2012).
16. R. M. H. Bilal, M. A. Naveed, M. A. Baqir, M. M. Ali, and A. A. Rahim, “Design of a wideband terahertz metamaterial absorber based on Pythagorean-tree fractal geometry,”Optical Materials Express, vol. 10, no. 12, p. 3007, 2020.
17. J. Wang, T. Lang, T. Shen, C. Shen, Z. Hong, and C. Lu, “Numerical study of an ultra-broadband all-silicon terahertz absorber,” *Appl. Sci.*, vol. 10, no. 2, p. 436, Jan. 2020.
18. B.-X. Wang, C. Tang, Q. Niu, Y. He, and R. Chen, “A broadband terahertz metamaterial absorber enabled by the simple design of a rectangular-shaped resonator with an elongated slot,” *Nanosc. Adv.*, vol. 1, no. 9, pp. 3621–3625, Sep. 2019, doi: 10.1039/c9na00385a.
19. M. Rahmanzadeh, H. Rajabalipanah, and A. Abdolali, “Multilayer graphene-based metasurfaces: Robust design method for extremely broadband, wide-angle, and polarization-insensitive terahertz absorbers,” *Appl. Opt.*, vol. 57, no. 4, p. 959, Feb. 2018, doi: 10.1364/ao.57.000959.
20. H.-F. Zhang, J.-X. Liu, J. Yang, H. Zhang, and H.-M. Li, “A polarization insensitive broadband terahertz absorber with a multilayer structure,” *Results Phys.*, vol. 11, pp. 1064–1074, Dec. 2018, doi: 10.1016/j.rinp.2018.11.010.
21. H. Liu, Z.-H.Wang, L. Li, Y.-X. Fan, and Z.-Y. Tao, “Vanadium dioxide assisted broadband tunable terahertz metamaterial absorber,” *Sci. Rep.*, vol. 9, no. 1, pp. 1–10, Dec. 2019, doi: 10.1038/s41598-019-42293-9.
22. C. Shi *et al.*, “Compact broadband terahertz perfect absorber based on multi-interference and diffraction effects,” *IEEE Trans. THz Sci. Technol.*, vol. 6, no. 1, pp. 40–44, Jan. 2016, doi: 10.1109/TTHZ.2015.2496313.
23. G. Deng, J. Yang, and Z. Yin, “Broadband terahertz metamaterial absorber based on tantalum nitride,” *Appl. Opt.*, vol. 56, no. 9, p. 2449, Mar. 2017, doi: 10.1364/ao.56.002449.
24. X. Liu, Q. Zhang, and X. Cui, “Ultra-broadband polarization independent wide-angle THz absorber based on plasmonic resonances in semiconductor square nut-shaped metamaterials,” *Plasmonics*, vol. 12, no. 4, pp. 1137–1144, Aug. 2017, doi: 10.1007/s11468-016-0368-1.
25. J. Yang *et al.*, “Broadband terahertz absorber based on multi-band continuous plasmon resonances in geometrically gradient dielectric loaded graphene plasmon structure,” *Sci. Rep.*, vol. 8, no. 1, pp. 1–8, Dec. 2018, doi: 10.1038/s41598-018-21705-2.

26. G. Varshney, “Wideband THz Absorber: By Merging the Resonance of Dielectric Cavity and Graphite Disk Resonator,”IEEE Sensors Journal, vol. 21, no. 2, pp. 1635–1643, 2021.
27. G. Varshney, “Reconfigurable graphene antenna for THz applications: A mode conversion approach,” Nanotechnology, vol. 31, no. 13,Mar. 2020, Art. no. 135208, doi: 10.1088/1361-6528/ab60cc.
28. M. Walther, D. G. Cooke, C. Sherstan, M. Hajar, M. R. Freeman, and F. A. Hegmann, “Terahertz conductivity of thin gold films at the metal insulator percolation transition,” Phys. Rev. B, Condens. Matter, vol. 76, no. 12, pp. 1–9, Sep. 2007, doi: 10.1103/PhysRevB.76.125408.
29. X.-R. Kong, H.-F. Zhang, and R.-N. Dao, “A tunable ultra-broadband THz absorber based on a phase change material,” J. Electron. Mater., vol. 48, no. 11, pp. 7040–7047, Nov. 2019, doi: 10.1007/s11664-019-07511-0.
30. T. K. Nguyen, P. T. Dang, I. Park, and K. Q. Le, “Broadband THz radiation through tapered semiconductor gratings on high-index substrate,” J. Opt. Soc. Amer. B, Opt. Phys., vol. 34, no. 3, pp. 583–589, 2017, doi: 10.1364/josab.34.000583
31. A. Alù, G. D’Aguanno, N. Mattiucci, and M. J. Bloemer, “Plasmonic brewster angle: Broadband extraordinary transmission through optical gratings,” Phys. Rev. Lett., vol. 106, no. 12, pp. 1–4, Mar. 2011, doi: 10.1103/PhysRevLett.106.123902.
32. M. Amin, M. Farhat, and H. Ba ˘ gcı, “An ultra-broadband multilayered graphene absorber,” *Opt. Express*, vol. 21, no. 24, p. 29938, Dec. 2013, doi: 10.1364/oe.21.029938
33. A. Fardoost, F. G. Vanani, A. Amirhosseini, and R. Safian, “Design of a multilayer graphene-based ultrawideband terahertz absorber,” *IEEE Trans. Nanotechnol.*, vol. 16, no. 1, pp. 68–74, Jan. 2017, doi: 10.1109/ TNANO.2016.2627939
34. J. Yang *et al.*, “Broadband terahertz absorber based on multi-band continuous plasmon resonances in geometrically gradient dielectric loaded graphene plasmon structure,” *Sci. Rep.*, vol. 8, no. 1, pp. 1–8, Dec. 2018, doi: 10.1038/s41598-018-21705-2.

Figures

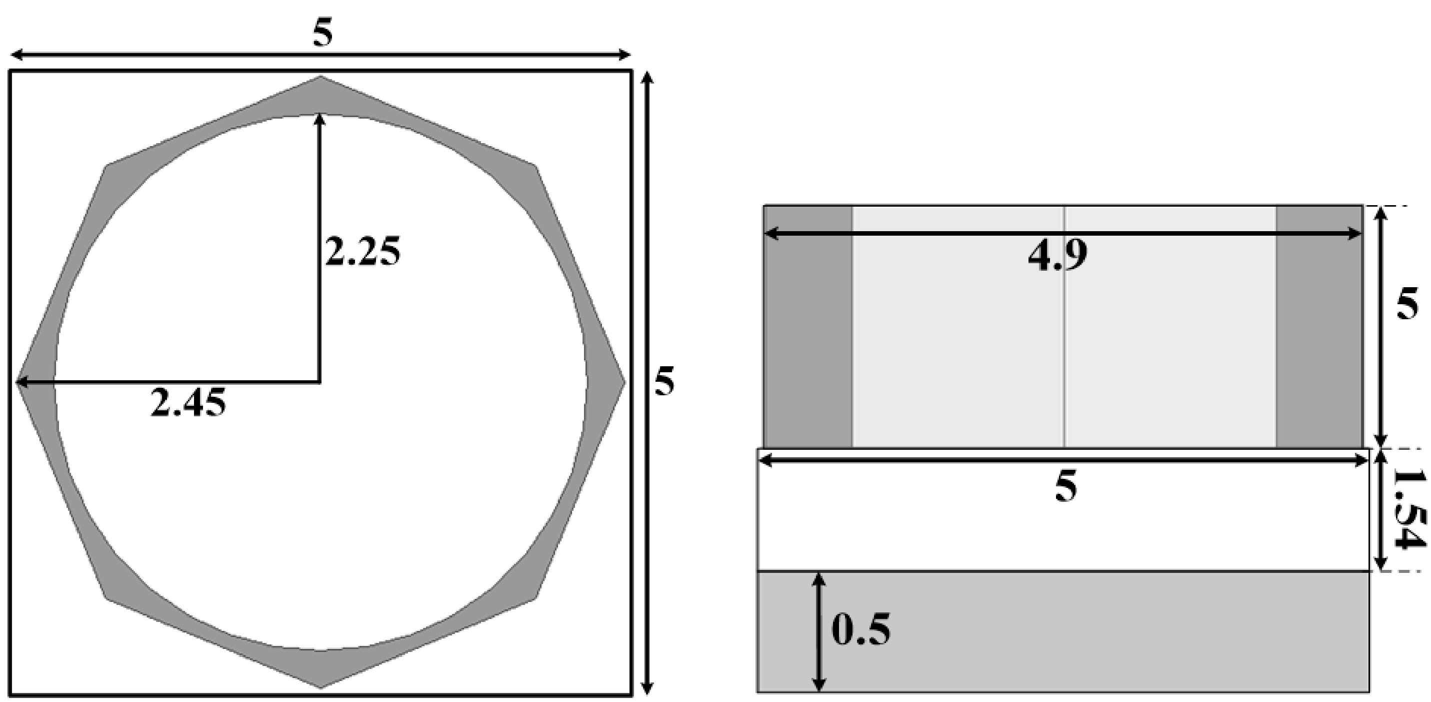

(a) (b)

Figure 1

Geometry of proposed absorber (a) top view, (b) side view (all dimensions are in μm)

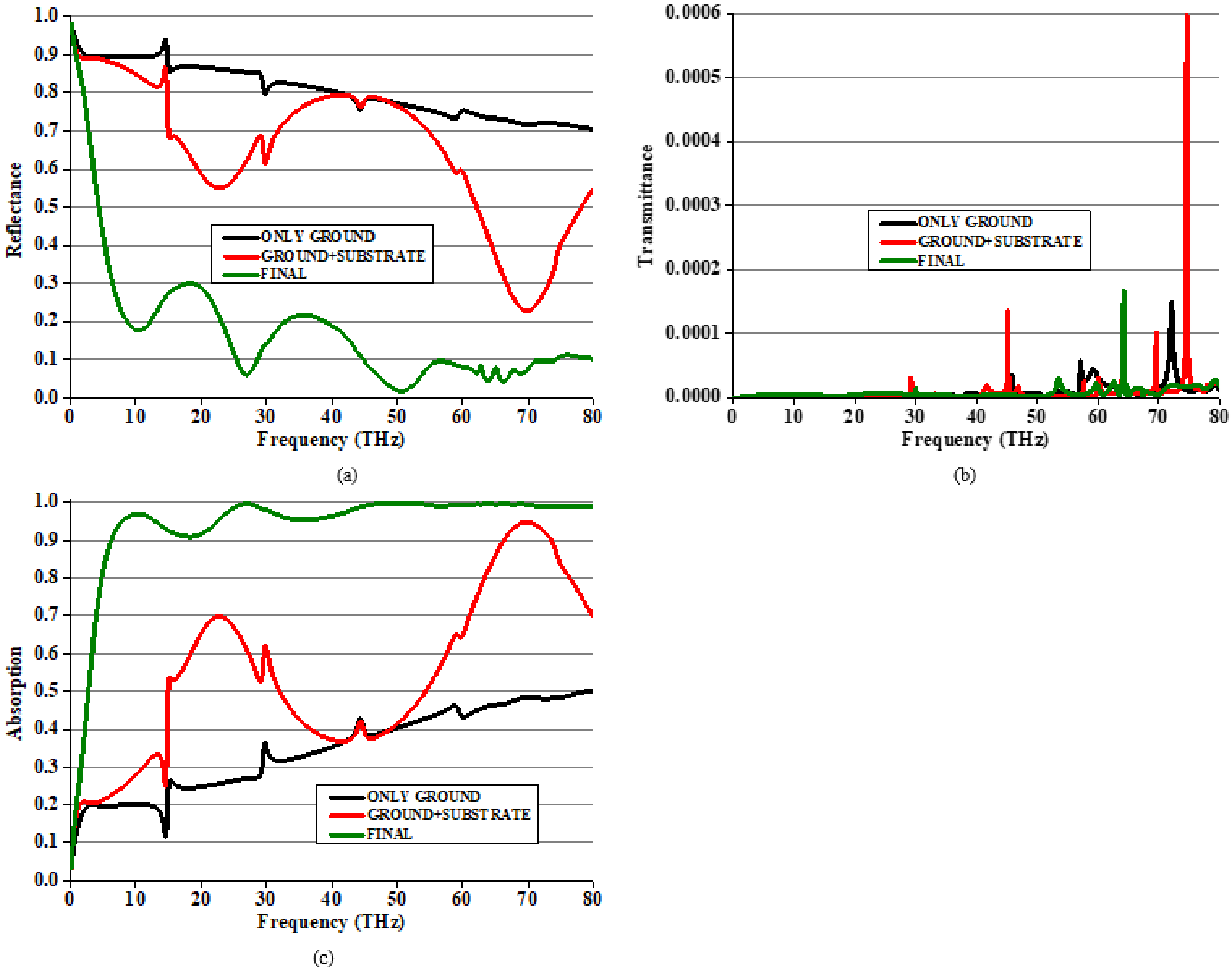

Figure 2

Performance of design stages (a) reflectance magnitude, (b) transmittance magnitude and (c) absorption

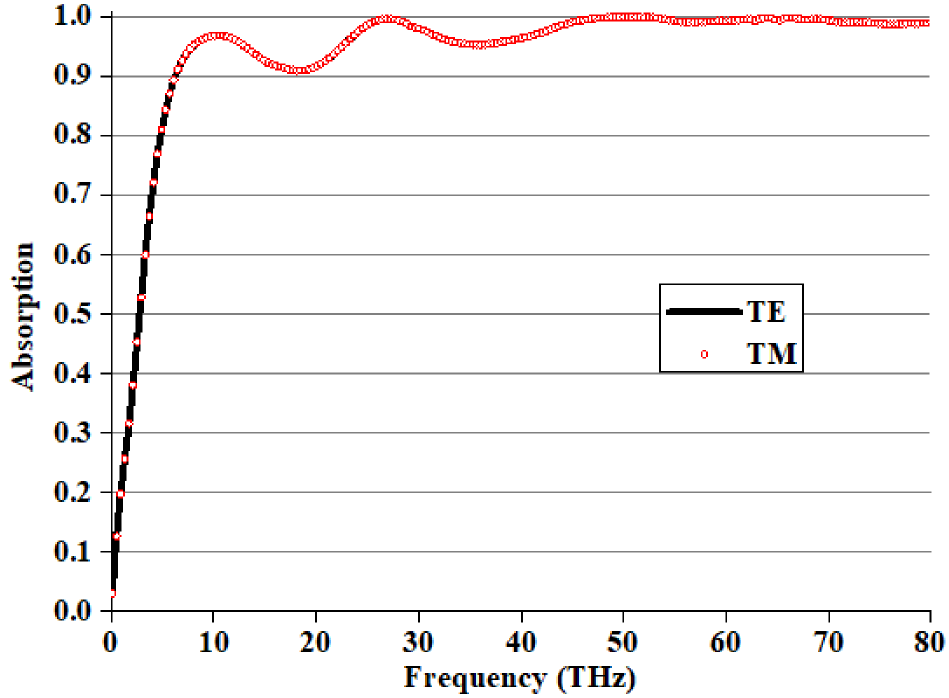

Figure 3

Absorption in TE and TM modes

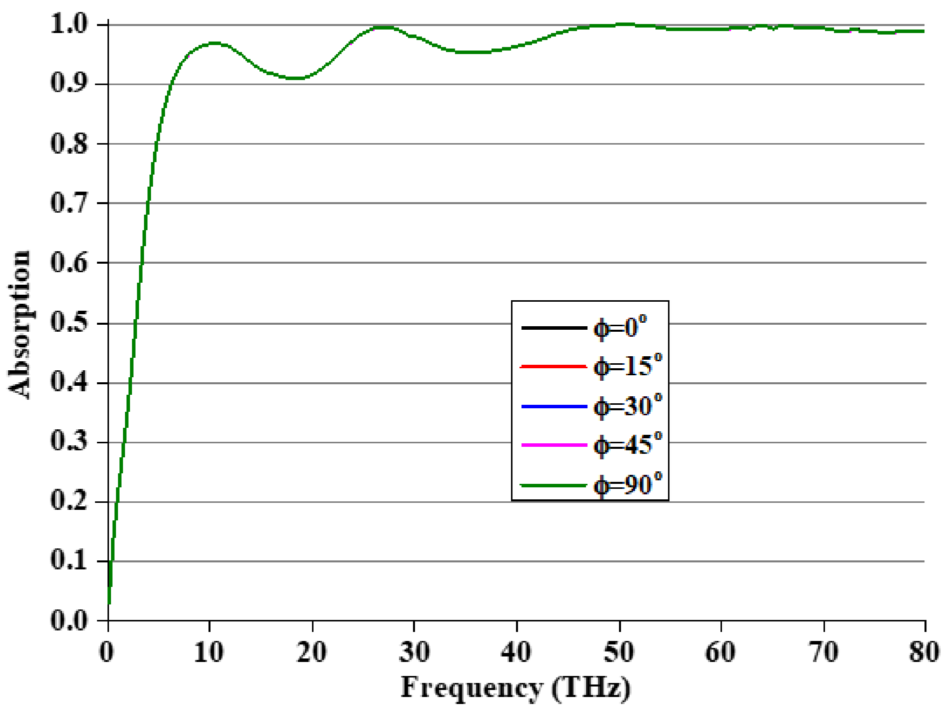

Figure 4

Absorption of proposed absorber with variations in polarization angle

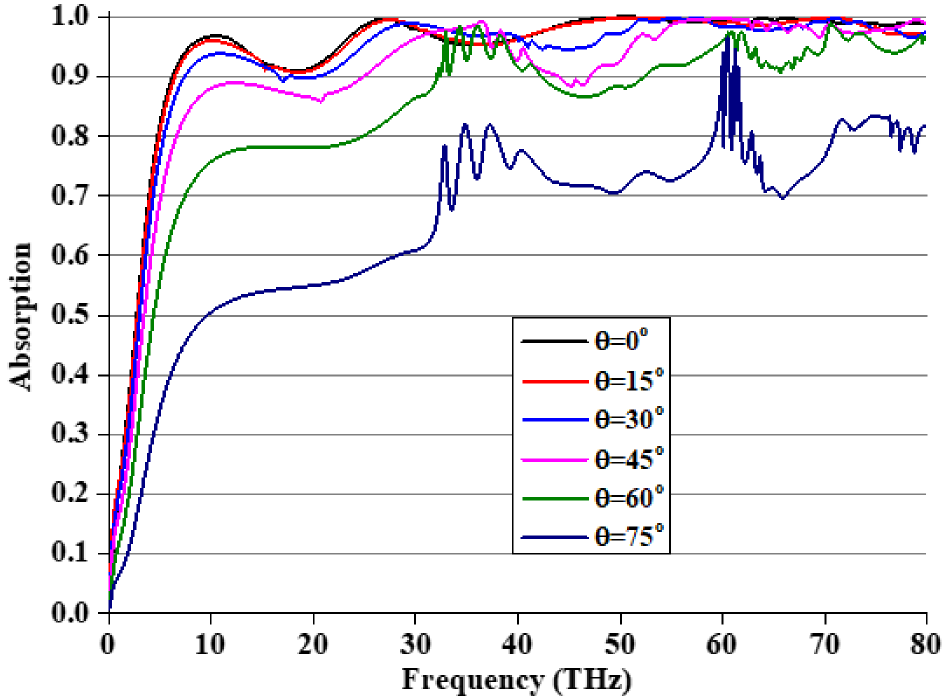

Figure 5

Absorption of proposed absorber with variations in incidence angle in TE mode

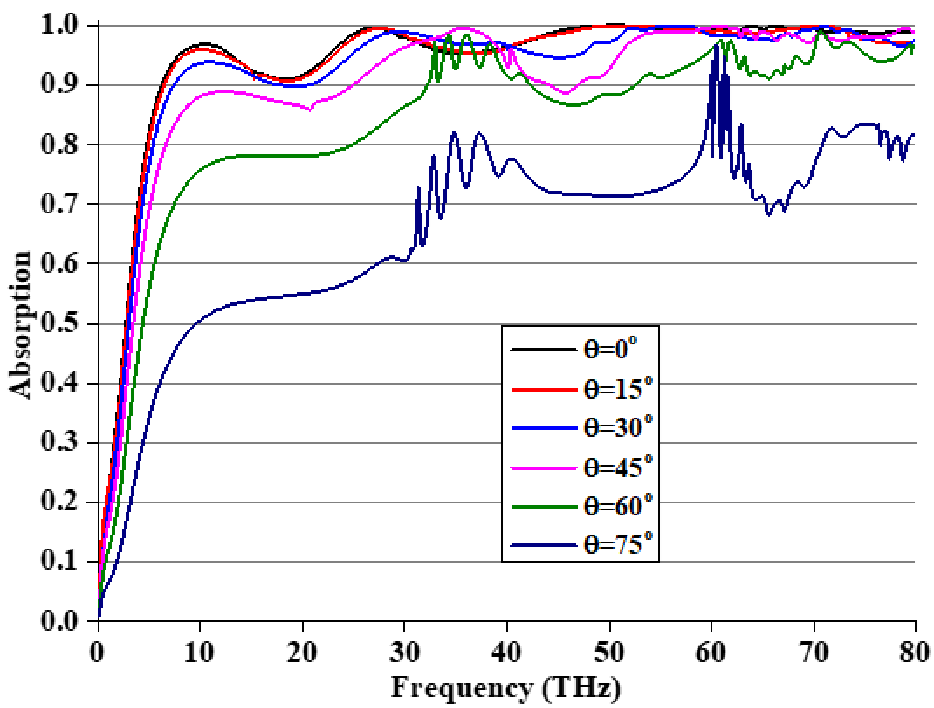

Figure 6

Absorption of proposed absorber with variations in incidence angle in TM mode